EPJ Web of Conferences **75**, 05012 (2014)
DOI: 10.1051/epjconf/ 20147505012

Lithography-free synthesis of nanostructured cobalt on Si (111) surfaces: structural and magnetic properties

W. Bounour-Bouzamouche[1,4], S. M. Chérif[1a], S. Farhat[1], Y. Roussigné[1], C.P. Lungu[2], F. Mazaleyrat[3] and M. Guerioune[4]

[1]LSPM (CNRS-UPR 3407), Université Paris 13, 99 avenue Jean-Baptiste Clément, 93430 Villetaneuse, France
[2]NILPR, 409, Magurele,JudIlfov, 077125, Bucharest, Romania
[3]SATIE, ENS Cachan, 61 Avenue du Président Wilson 94235 Cachan Cedex, France
[4]LEREC, Université de Annaba, BP12 – 23000, Algeria.

Abstract. We illustrate the concept of lithography-free synthesis and patterning of magnetic cobalt in the nanometric scale. Our elaboration method allows fabricating 2D architectures of cobalt and cobalt silicide onto silicon (111) surfaces. A continuous cobalt layer of 1, 3 and 10 nm thickness was first deposited by using thermoionic vacuum arc (TVA) technology and then, thermally annealed on vacuum at temperatures from 450° C to 800° C. Surface structure was analyzed by atomic force and field emission-scanning electron microscopies. Above 750° C, regular triangular shape cobalt nanostructures are formed with pattern dimensions varying between 10 and 200 nm. Good control of shape and packing density could be achieved by adjusting the initial thickness and the substrate temperature. Magnetic properties were investigated by means of vibrating sample magnetometer (VSM) technique. The evolution of the coercive field versus packing density and dimensions of the nanostructures was studied and compared to micromagnetic calculations. The observed nanostructures have been modelled by a series of shapes tending to a fractal curve.

1 Introduction

Thin magnetic materials have been intensively investigated due to their interesting physical properties and technological applications. Indeed, in modern nanoelectronics, the development of ultrahigh-density magnetic storage materials with good quality of interfaces are needed [1]. A great amount of research has been devoted to the study of magnetic surfaces and interfaces as well as step induced anisotropies in ferromagnetic ultrathin films [2-5]. The growth of magnetic materials on semiconductors as silicon (100) and (111), GaAs, MgO, etc… has opened new perspectives for novel magnetic thin film devices [6]. However, the reaction of deposited 3d transition metals with silicon substrate hinders the development of magnetic structures in the ultrathin range [7-9]. Cobalt is widely used in magnetic recording media while silicon is the most important substrate in semiconductor industry. The reaction Co/Si generally leads to formation of a silicide. As the reaction temperature increases, the silicide stoichiometry becomes more silicon rich. These compounds formed during the deposition can be magnetic and induce parasite contribution. The growth of cobalt on a silicon surface followed by different annealing below 400° C leads to the formation in layers of three types of cobalt silicide: Co_2Si, CoSi and $CoSi_2$ [13]. These silicides have been extensively studied because of their excellent electrical properties (Schottky barrier and high mean free path of electrons). Cobalt deposited on annealed rubrene/Si(100) forms Co islands in triangular shapes [14]. Because of the clustering and pinhole formation for annealed rubrene layer, the formation of a Co/Si(100) interface was found to be crucial for the occurrence of the pyramid-like nanostructure with an hcp stacking of the Co layer. In this paper, we present the structural and magnetic properties of Co thin films (1, 3 and 10 nm-thick) first deposited on Si(111) and then, thermally annealed on vacuum at temperatures ranging from 450°C to 800°C. Atomic force microscopy (AFM) and field emission scanning electron microscope (FE-SEM) were utilized to characterize the surface morphologies. The magnetic properties of the Co samples were analyzed with a vibrating sample magnetometer (VSM) at room temperature. For annealed Co/Si(111) films submitted to hydrogen plasma, we observe an enhancement of the coercive field, compared to the as deposited and annealed films, which could be related to the formation of Co islands in triangular shapes. Similar behavior has been reported for Co deposited on annealed rubrene/Si(100) [14]; the observed enhancement of the squareness of magnetization curve for Co overlayers was attributed to formation of Co islands in triangular shapes.

[a] cherif@univ-paris13.fr

2 Sample and experimental set up

In the present work, three cobalt thin films of thicknesses t of 1, 3 and 10 nm respectively were deposited onto silicon (111) substrates, using thermionic vacuum arc (TVA) method [10]. The thin cobalt films were first thermal annealed in a vacuum chamber at a pressure of 2×10^{-6} mbar at temperature of 750 °C or 800°C.
We used a 10 cm diameter silica bell jar low pressure reactor activated by a microwave electric field (figure 1). Then, samples were hydrogenated with pure hydrogen plasma (90 sccm) during 10 to 60 minutes. The Co/Si substrate is held in a resistance boat made in molybdenum and electrically annealed. During the process, temperature was controlled by infrared pyrometer. The reactor utilizes 1.2 kW SAIREM microwave generator operating at 2.45 GHz. The electromagnetic waves are generated, guided in a rectangular wave guide and applied inside the cavity delimited by Faraday cage.

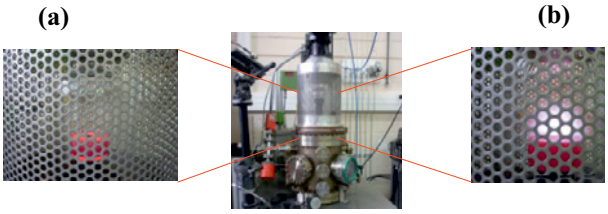

Fig.1. (Color on line) Plasma enhanced chemical vapour deposition, PECVD Bell jar reactor, (a) during thermal annealing, b) during plasma treatment.

The morphology of the surface of the samples was observed by means of field emission gun scanning electron microscopy (FE-SEM, SUPRA 40VP, ZEISS) and atomic force microscopy (AFM D3100, Nanoscope NS3). The static magnetic properties were studied using vibrating sample magnetometer (VSM). We used a Lake Shore 7404 VSM which shows a high sensitivity (10^{-7} emu) and then enables to record extremely low magnetic signal.

3 Results and discussion

3.1 Effect of film thickness

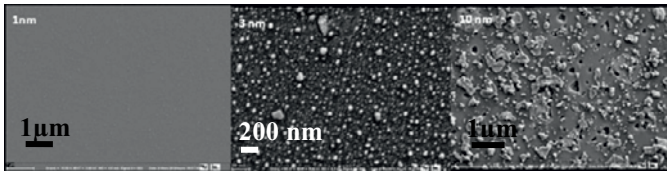

Fig.2. FE-SEM images of the films (a) 1 nm, (b) 3 nm and (c) 10 nm, after thermal treatment at 750° C

Figure 2 shows FE-SEM images of cobalt islands formed from film of 1 nm and 3 nm on the silicon substrate after the thermal treatment at 750°C. For the 1 nm film, the particles have a spherical-like shape and are isolated from each other. Diameter distribution of islands is homogeneous. With the increase of thickness, t=3 nm, a slight modification is noticed; the islands diameter increases and their reorganization is less marked. For the thicker film t=10 nm, we note a distinct change in the nanostructuring of the initial Co layer; the nanoparticles nucleate to form clusters and defects develop in the film. Nanoparticles average diameters of 34 nm and 49 nm have been obtained for the1 nm and 3 nm-thick films, respectively. The FEG-SEM images clearly show that the use of pre-treatment step does not give individual nanoparticles as can be seen for the 10 nm-thick cobalt. This results show that catalyst film thickness clearly affects the subsequent particle size, as has been previously demonstrated [15].

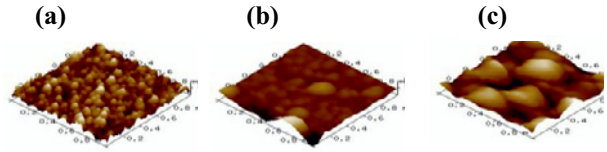

Fig.3. (Color on line) 1 µm×1 µm AFM images of the Co/Si(111) films: (a) 1 nm, (b) 3 nm and (c) 10 nm

From Figure 3, one can notice that the measured roughness mean square (RMS), obtained from AFM images, is well correlated with the original thickness. For the 3 and 10 nm-thick films, thermal annealing increases, slightly the RMS; we can attribute this fact to the agglomeration of the initial particles into higher size domains. We observe clearly that the diameter of the cobalt islets decreases with thickness of the catalyst. The thinnest cobalt sample (1 nm) has homogeneous particles and an average roughness about 0.8 nm. For the 3 nm-thick film, we measure an average roughness of about 3.3 nm, while the one determined for the 10 nm-thick sample is about 17 nm. Similar correlation between the film thickness and the size of catalyst nanoparticles formed after thermal annealing has already been reported [11-13].

3.2 Effect of treatment temperature

In order to study the effect of the annealing temperature on the surface morphology, we compared sample behaviour for non-treated film and annealed at 450 °C and 650 °C respectively. Figure 4 shows the evolution of the surface morphology in the case of the 3 nm-thick film. As deposited film shows a succession of dark patches and bright fractal like islands. When annealed at 450 °C, the bright domains transform to small clusters of average size of 100 nm. This could be attributed to the interaction at high temperature of cobalt with the (111) surface silicon atoms. The Co clusters seems to be uniform. This morphology changes with annealing time and treatment, probably due to the observed fractal like structure. This behaviour is in accord with the results reported by Fu *et al.* [13]. Increasing the annealing

temperature to 650 °C increases the size of these triangles to an average value of 200 nm.

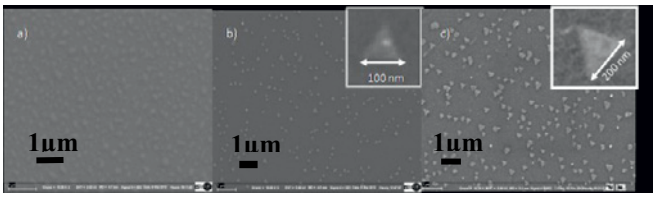

Fig.4. FE-SEM images of the 3 nm cobalt film (a) without thermal annealing, (b) annealed at 450 °C and (c) annealed at 650 °C. The size of the triangles increases with annealing temperature.

3.3 Magnetic properties

Hysteresis loops have been recorded at room temperature for all the samples. We report below the results for the 3 nm-thick as deposited film, the annealed one at 650°C and the one also submitted to a H_2 plasma treatment (Fig. 6), with an external field applied in the plane of the samples. The as deposited film (not shown) exhibits a low coercive field H_c. After annealing treatment at 650°C, sparse Co nanometer sized triangles are formed on the surface of the sample (Fig. 4(c)). The corresponding loop exhibits a higher coercive field of about 7 mT (70 Oe) (Fig. 6(a)). When submitted to a H_2 plasma treatment, the surface shows a more complex morphology with close islands and clusters covering the surface as shown in Figure 5. We observe a very large increase of H_c up to 150 mT (1500 Oe) (Fig. 6(b)).

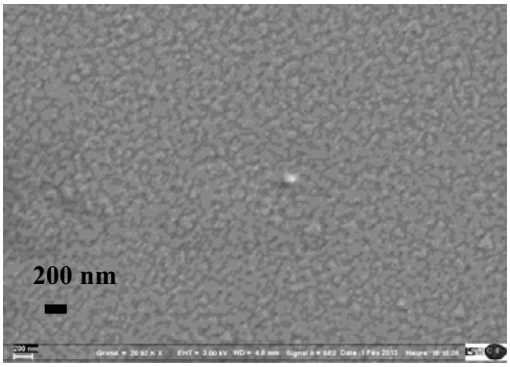

Fig.5. FE-SEM images of the 3 nm cobalt annealed at 650 °C after H_2 plasma treatment during 20 minutes.

An enhancement of the squareness is noticed after hydrogen plasma treatment. The observed curvature of the hysteresis loops can be due to the distribution of triangle dimensions, inhomogeneities, dipolar interactions between islets and to the structural defects. Thus, the magnetization reversal does not occur exactly at the coercive field value but there is a switching field distribution. It is to notice that increasing the plasma treatment from 20 minutes to 1 hour does not modify the measured hysteresis loop. The formation of Co islands in triangular shapes was found to play an important role on the enhancement of the squareness of magnetization curve of Co deposited on annealed rubrene/Si(100) [14].

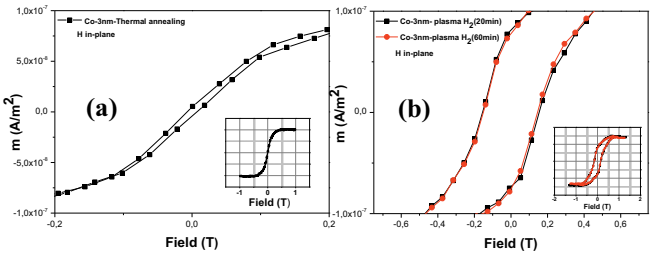

Fig.6. (Color on line) In-plane hysteresis loops for (a) annealed sample at 650°C, (b) sample submitted to H_2 plasma treatment for two different times: 20 minutes (black symbols) and 60 minutes (red symbols). Higher coercive field is observed for the sample under H_2 plasma treatment. The insets show the loops within the magnetic field range [- 1 T; 1 T].

In order to qualitatively describe the magnetization behavior, numerical simulations have been performed using the OOMMF software to find equilibrium magnetization distributions for different external magnetic fields: the 2D solver was utilized with a cell size of 5 nm and the usual Co bulk material parameters: saturation magnetization $M_s = 1400\times10^3$ A/m (1400 emu/cm^3), exchange constant $A = 13\times10^{-12}$ J/m (1.3×10^{-6} erg/cm).

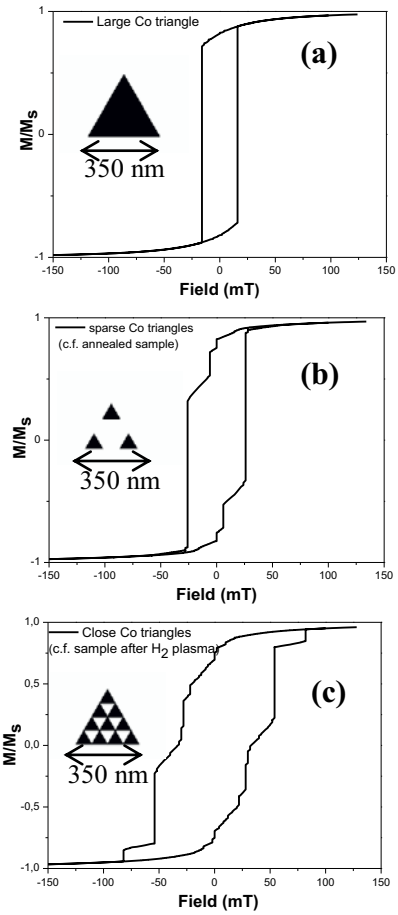

Fig.7. Calculated in-plane hysteresis loops for a large triangle (a), sparse small triangles (b) and close small triangles (c). The thickness is 5 nm and the side is 350 nm.

We considered 3 cases for a given thickness of 5 nm, equal to the cell size: a large triangle (size 350 nm), sparse and close small triangles (size 87.5 nm). These 3

cases roughly refer to as deposited (Fig. 7(a)), the annealed (Fig. 7(b)) and the H_2 plasma treated films (Fig. 7(c)), respectively.

The small triangles, weakly coupled, display a higher coercive field than the large triangle's one. In fact, in a large triangle a multi-domain magnetization structure is allowed facilitating the magnetization reversal initiated near the edges. When the small triangles are largely coupled, either by exchange through direct contacts or by dipolar field, the magnetization reversal involves neighboring triangles yielding a complex reversal process. The high density of triangles induces large dipolar fields because each triangle is not large enough to support a multi-domain magnetization structure as exhibited in Figure 8. Thus the energy cost for magnetization reversal is high yielding a large coercive field.

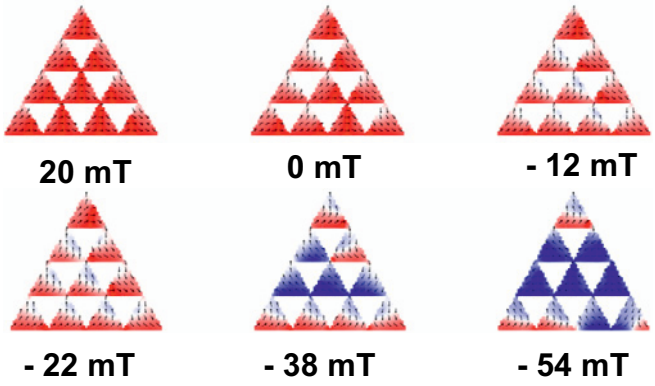

Fig.8. (Color on line) Calculated magnetization configurations for the close small triangles for different values of the applied magnetic field. The high density of triangles induces large dipolar fields. Energy cost for magnetization reversal is thus high, yielding a large coercive field.

The simulations qualitatively reproduce the experimental trends, however to get more insights about the magnetization behavior of the cobalt/Si(111) films submitted to annealing and hydrogen plasma treatment, one has to consider more complex shapes tending to a real fractal curve and to take into account the effect of structural and composition changes. This work is under investigation and will be presented elsewhere.

5 Conclusions

Cobalt thin films of thickness of 1, 3 and 10 nm were deposited onto silicon (111) substrates, using thermionic vacuum arc (TVA) method. Initial film thickness influences the organisation of the islands or clusters obtained after a thermal treatment at 750°C: nanoparticles of average diameters of 34 nm and 49 nm were obtained for the1 nm and 3 nm-thick films, respectively, while for the 10 nm-thick film, we note a distinct change of the morphology of the initial Co layer; the nanoparticles nucleate to form clusters and defects develop in the film. A direct correlation between the film thickness and the size of the nanoparticles formed after thermal annealing is pointed out. The modification of the surface morphology after annealing and plasma treatment indeed strongly influences the magnetic response of the investigated films. The formation of Co islands in triangular shapes is found to play a key role in the enhancement of the coercive field comparing to the as deposited film, as qualitatively confirmed from the micromagnetic calculations.

Acknowledgments

We thank C. Porosnicu and A. Anghel for the help in the elaboration of the as deposited Co films. We also acknowledge support from the Laboratory of Excellence SEAM of University Sorbonne Paris Cité (USPC).

References

1. C. Vaz, J. Bland, G. Lauhoff, *Magnetism in ultrathin film structures*, Rep. Prog. Phys**71**, 056501 (2008).
2. B. Engel, M. Wiedmann, R. Van Leeuween, C. Faclo, Phys.Rev. B **48**, 9894 (1993).
3. R.K. Kawakami, E.J. Escorcia-Aparicol, Z.Q. Qui, Phys. Rev. Lett. **77**, 2570 (1996).
4. B. Heinrich, S.T. Purcell, J.R. Dutcher, K.B. Urquhart, J.F. Cochran, A.S. Arrot., Phys. Rev. B **38**, 12879 (1988).
5. A. Berger, U. Linke, H.P. Open, Phys. Rev. Lett. **68**, 839 (1992).
6. M.O. Aboelfotoh, A.D. Marwick, J.L. Freeouf, Phys. Rev. B **49**, 10753 (1994).
7. J. Derrien, M. De Crescenzi, E. Chainet, C. D'Anterruches, C. Pirri, G. Gewinner, Phys. Rev. B **36**, 6681(1987).
8. J.S. Tsay, C.S. Yang, Y.D. Yao, Jpn. J. Appl. Phys. **37**, 59768 (1998).
9. C.-A. Chang, Appl. Phys. Lett. **57**, 297 (1990).
10. C. P. Lungu, I. Mustata, V. Zaroschi, A. M. Lungu, A. Anghel, P. Chiru, M. Rubel, P. Coad, G. F. Matthews, Phys. Scripta **2007**,T128, 157 (2007).
11. A. Rizzo, R. Rossi, M.A. Signore, E. Piscopiello, L. Capodieci, R.Pentassuglia, T. Dikonimos, R. Giorgi, Diam. Relat. Mater. **17**, 1502 (2008).
12. R. K. Garg, S. S. Kim, D. B. Hash, J. P. Gore, T. S. Fisher, J. Nanos. Nanotec. **8**, 3068 (2008).
13. T.Y. Fu, J.S. Tsay, M.H. Lin, Y.D. Yao, J. Magn. Magn. Mater. **304**,128 (2006).
14. C.Y, Hsu, C.H.T. Chang, W.H. Chen, J.L. Tsai, J.S. Tsay, J. Alloys Comp. **576**, 393 (2013).
15. S. Hofman, M. Cantoro, B. Kleinsorge, C. Casiraghi, A. Parvez, J. Roberston, C. Ducati, J. Appl. Phys. **98**, 034308 (2005).